A Moment-Based Study on the Impedance Effect of Mutual Coupling for VLF Umbrella Antenna Arrays

Bin Li[*], Chao Liu, and Hua-Ning Wu

Abstract—The mutual coupling between very low frequency (VLF) antenna elements is an important factor affecting the radiation performance of umbrella antenna arrays. This study evaluates the factors influencing the mutual coupling between the elements of an umbrella antenna array. We develop a mutual coupling analysis method for calculating the input impedances of a VLF antenna based on the impedance effect of mutual coupling. The radiation resistance of the VLF umbrella antenna can be obtained using numeric integral from Method of Moments (MoM) solution. Using the FEKO simulation software, a model of a trideco-tower umbrella antenna array is established. The electrical parameters of the VLF umbrella antenna array on inhomogeneous ground are calculated for both single and dual feeding modes. The impedance characteristics of the umbrella antenna arrays are also simulated for different array inter-element spacings on homogeneous ground. Representative numerical results are reported and discussed to assess the mutual coupling effect of the proposed method in comparison with full-wave simulations.

1. INTRODUCTION

VLF communication has been adopted widely for navigation, time broadcasting, and underground communication [1–3]. Generally, a practical VLF transmitting antenna is an electrically-small antenna (ESA), which is placed on a large-scale ground screen [4, 5]. In order to improve the current distribution of the vertical antenna, a top load is applied to a VLF umbrella antenna. It is well known that the optimization of the antenna's quality factor and radiation resistance is not a significant function of the antenna's geometry or total wire length [6]. However, it is obvious that improving the antenna's performance requires that the antenna's volume and effective height are as large as possible. Compared with other VLF antennas, such as T-type antennas and whip antennas of equal height, the umbrella antennas have the advantages of small reactance and high radiation efficiency [7–9]. At present, an umbrella antenna array is the main antenna model of shore-based VLF communications.

Given previous VLF antenna array design considerations, the mutual coupling [10] between the array elements is inevitable. It has been demonstrated that power can be transferred between two or more self-resonant antennas, which are placed in close proximity and are strongly coupled [11]. Since an umbrella antenna with a complex structure operates under high current and voltage, the mutual coupling between the VLF antenna elements is an important factor affecting the radiation performance of the umbrella antenna array. There are many studies focused on the mutual coupling effects of wire antennas using numerical analysis [12–18]; however, the input impedance has not received sufficient attention. In order to assess the performance of a VLF antenna array, the mutual coupling effect must be considered in the design of a VLF antenna array. When the VLF antennas are strongly coupled, the input impedance of the VLF transmitting antenna also varies depending on the operating modes and the space between the coupled antennas. This study focuses on the determination of the mutual

coupling for a VLF transmitting antenna array based on the input impedance of each antenna element. At present, there is a lack of published information regarding the input impedance of a VLF umbrella antenna, especially with regard to simulations and calculation methods. Therefore, this study proposes an impedance analysis method based on the induction electromotive force and calculates the input impedance of the coupled VLF umbrella antenna by applying a MoM solution. Solving the input impedance provides an approximate solution for the mutual coupling.

This paper is organized as follows. Section 2 describes the numerical calculations for determining the impedance effect of the mutual coupling and the MoM calculations for the VLF umbrella antenna array. In Section 3, we briefly introduce the model of the VLF umbrella antenna array in the FEKO software. In Section 4, we present the simulation results and illustrate the mutual coupling effects of the VLF umbrella antenna array. The conclusions of this paper are presented in Section 5.

2. NUMERICAL CALCULATIONS FOR THE UMBRELLA ANTENNA ARRAY

2.1. The Impedance Effect of Mutual Coupling

At present, the methods for analyzing the coupling between the array elements in an array antenna include [19] the open circuit voltage method [20], active pattern method [21], and induced electromotive force method [22, 23]. The open circuit voltage method uses mutual impedance to assess the mutual coupling, by obtaining the open-circuit voltage and short-circuit current. As the spacing of arrays is less than half of the wavelength, it is inaccurate for the active pattern method to study the mutual coupling of the VLF antenna arrays. The induced electromotive force method calculates the impedances by impedance matrix. Both the open circuit voltage method and induced electromotive force method are applicable to the mutual coupling of the VLF antenna array. However, the computational accuracy of the open circuit voltage method and induced electromotive force method is not as good as the MoM. Compared with other band analyses concentrating on the gain and standing-wave ratio (SWR), the performance of the VLF antenna array is mainly reflected in the input impedance and the output power. Therefore, we can study the mutual coupling of the VLF umbrella antenna array from the perspective of impedance.

There are three approaches to achieve the mutual coupling of the VLF antenna. One approach is the direct mutual coupling between the antenna array elements. In addition to its own radiation impedance, the electromagnetic wave radiated from the other array elements excites the induced current, which radiates back to form induced impedance. Thus, a mutual radiation of induction forms a direct coupling. The second approach is the indirect coupling from the surrounding environment of the antenna, and the body of the support tower is the main scatter of the umbrella antenna. The third approach is the simultaneous operation of the two umbrella arrays whereby the feeding network provides the coupling path and based on an optimal feeding mode and impedance matching. Due to the long wavelength, the feeding line can be seen as a feeding point. The coupling degree of the feeding network can be negligible. Due to the existence of the coupling effect, the radiation impedance is divided into two parts, self-radiation impedance and induction impedance [24]. The self-impedance is given as:

$$Z_{ii} = R_{ii} + jX_{ii} \tag{1}$$

where R_{ii} is the self-resistance, and X_{ii} is the self-reactance. The self-impedance is the impedance of the isolated element without consideration of the environmental effects. Taking into account that the mirror image of the vertical antenna does not radiate power, the radiation resistance of the vertical antenna is half of the free space symmetric oscillator. Thus, the resistance and reactance of the self-impedance of the ith monopole antenna on a perfect conducting ground can be obtained by:

$$R_{ii} = 160\pi^2 \left(\frac{h_{ei}}{\lambda}\right)^2 \tag{2}$$

$$X_{ii} = -jW_{vi}\text{ctg}\left(kh_i'\right) \tag{3}$$

where W_{vi} denotes the characteristic impedance of the ith monopole antenna, h_{ei} the effective height of the ith array element, h_i' the equivalent height of the whip antenna with the characteristic impedance of W_{vi}, and k the wave number. The mutual impedance, which can be obtained by the induction

electromotive force method is the inductive impedance when the amplitude and phase of each antenna element are the same. Taking the two element arrays as an example, the expressions of mutual resistance and mutual reactance can be respectively expressed as follows:

$$R_{12} = \frac{60h_{e1}h_{e2}}{kd_{12}^3} \left[kd_{12}\cos(kd_{12}) - \left(1 - k^2d_{12}^2\right)\sin(kd_{12}) \right] \tag{4}$$

$$X_{12} = \frac{60h_{e1}h_{e2}}{kd_{12}^3} \left[kd_{12}\sin(kd_{12}) + \left(1 - k^2d_{12}^2\right)\cos(kd_{12}) \right] \tag{5}$$

where d_{12} is the distance between the bases of the two center towers. Accordingly, the input impedance of the two arrays can be evaluated without any simulation. With regard to an ESA, h_0 is much smaller than λ. The arrays are strongly coupled prior to touching each other's the minimum hypothetical spheres [13]. Then, the effective height of the ith array element can be simplified as:

$$h_{ei} \approx h\left(1 - \frac{h}{h_0}\right) \tag{6}$$

Due to the strongly coupling of the closely located ESAs, the addition theorem remains a valid method to study the mutual coupling between the ESAs of the transmitting system. As shown in Figure 1(a), in the mutual coupling model of two array elements, the total voltage can be expressed as:

$$\begin{cases} V_1 = Z_{11}I_1 + Z_{12}I_2 \\ V_2 = Z_{21}I_1 + Z_{22}I_2 \end{cases} \tag{7}$$

The mutual impedance can be obtained by respectively measuring the port impedance of the other antenna element when the circuit of antenna element is open or shorted. This is known as $Z_{12} = Z_{21}$ based on the reciprocity theorem. When we divide the Equation (7) by the loop current I_1 and I_2, the input impedance can be obtained as follows:

$$\begin{cases} Z_1 = Z_{11} + me^{j\psi}Z_{12} \\ Z_2 = Z_{22} + \dfrac{1}{m}e^{-j\psi}Z_{21} \end{cases} \tag{8}$$

where m denotes the current amplitude ratio of the antinode, and ψ denotes the difference in the current phase. The real part of the input impedance is the input resistance and the imaginary part is the input reactance.
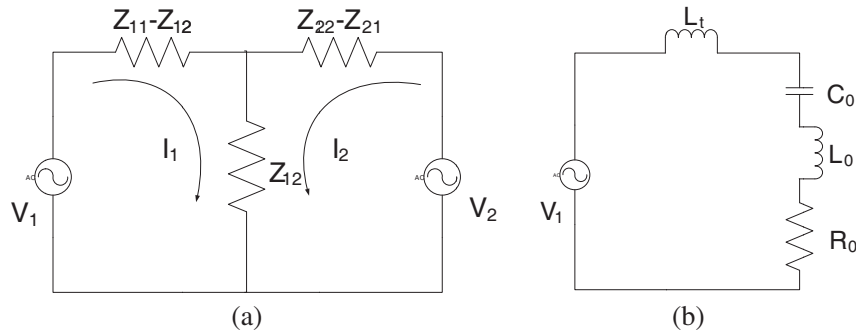
Figure 1. (a) The equivalent network analysis diagram to the arrays. (b) The equivalent circuit diagram to the antenna.

As shown in Figure 1(b), the VLF antenna can be equivalent to the RLC circuit, where L_t denotes the tuning inductance located in the helix house C_0 denotes the equivalent capacitance of the antenna, L_0 denotes the equivalent inductance of the antenna, and $R_0 \approx R_r + R_g$ denotes the input resistance of the antenna. R_r is the radiation resistance of the antenna, and R_g is the resistance of ground loss which is the major loss of the VLF antenna. As for a VLF antenna, the transfer function can be expressed as:

$$G(s) = \frac{sR_rC_0 + 1}{sR_0C_0 + 1 + s^2L_tC_0} \tag{9}$$

Usually, the radiation resistance is simulated as the input resistance of the antennas on ground with perfect electrical conductance, which is related to the power capacity, stability and radiation efficiency of the system. The input resistance is obtained by $R_{in} = R_{11} + R_{12} + R_g$. The ground loss resistance consists of the magnetic field loss resistance and the electric field loss resistance [5]. The antenna efficiency is defined by $\eta = \frac{R_r}{R_{in}} \times 100\%$. When the input resistance is certain, reducing the loss resistance (tuning loss and ground loss) is an important way to improve the radiation efficiency of the antenna.

2.2. MOM Calculations for VLF Umbrella Antenna Array

Although VLF umbrella antenna arrays are huge in scale, their electric dimension is small. As a numerical analysis technique based on the frequency domain integral equation the MoM is a general method for solving linear equations of low frequency electromagnetic fields [25]. Essentially, the integral equation is transformed into a matrix equation represented by a series of base functions. Subsequently, the unknown term (e.g., the current value) of the operator equation is solved by means of elimination and inversion. Thus, the directional pattern and impedance can be calculated directly.

A coupled wire or thin wire antenna array is applicable to the integration theory. The current $I(s)$ along the wire satisfies the following electric field integral equation (EFIE) [4, 26–29]:

$$-\hat{s} \cdot E^i(r) = \frac{-j\eta}{4\pi k} \int_L I\left(s'\right) \cdot \left(k^2 \hat{s}' \cdot \hat{s} - \frac{\partial^2}{\partial s \partial s'}\right) g\left(r, r'\right) ds' \tag{10}$$

where $E^i(r)$ denotes the incident electric field, $g(r, r') = \exp(-jk|r - r'|)/|r - r'| \eta = \sqrt{\mu_0/\varepsilon_0}$, $k = \omega\sqrt{\mu_0 \varepsilon_0} r'$ denotes a point on the wire axis at s', and r denotes a point on the wire surface at s. s is the distance parameter along the wire axis at $r\hat{s}$ is its unit vector tangent to the wire axis. $|r - r'| \geq a$ and the integrand term is bounded. A straight line on a wire antenna can be divided by N segments as shown in Figure 2. Then, the current on the segment index i is expanded by an orthogonal pulse function or segmented sinusoidal base function:

$$I_i(s) = A_i + B_i \sin k(s - s_i) + C_i \cos k(s - s_i) \quad |s - s_i| \leq \Delta_i/2 \tag{11}$$

where s_i is the value of s at the center of segment i, and Δ_i is the length of segment i. Therefore, the solution Equation (10) can be expanded into a series expression in linear space, which is expressed by a linear independent base function.

$$-\hat{s} \cdot E^i(r_m) = \left(\frac{-j\eta}{4\pi k}\right) \sum_{i=1}^{N} a_i \int_{L_i} I_i\left(s'\right) \cdot \left(k^2 \hat{s}'_i \cdot \hat{s}_m - \frac{\partial^2}{\partial s \partial s'}\right) g\left(r_m, r'\right) ds' \quad m = 1, 2, \ldots, N \tag{12}$$

In order to convert the integral equation into a linear algebraic equation group, we choose the proper weight function to perform the inner product operation with the base function. Therefore, the inner product can be represented by:

$$\langle w_j, E^i(r) \rangle = jw A_l(j) \cdot \Delta j + \frac{\partial \varphi(m)}{\partial l} \Delta j \tag{13}$$

where $w_j = \Delta l_j \delta(j)$ is chosen as the weight function. $A_l(j)$ is the magnetic vector potential at the center of wire segment l, and $\varphi(m)$ is the electric scalar potential. As for thin wire, we can approximately
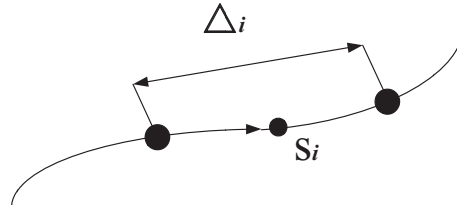
Figure 2. Segmentation of wire antenna.

calculate $\frac{\partial \varphi(m)}{\partial l}$ as follows

$$\frac{\partial \varphi(m)}{\partial l} \approx \frac{\varphi\left(\overset{+}{j}\right) - \varphi\left(\overset{-}{j}\right)}{\Delta l_j} \tag{14}$$

Substituting Eq. (14) into Eq. (13) yields the simplified expression

$$jwA_l(j) \cdot \Delta j + \left[\varphi\left(\overset{+}{j}\right) - \varphi\left(\overset{-}{j}\right)\right] = U(j) \tag{15}$$

According to Equation (15), one axis line of the umbrella antenna can be matched by adding and subtracting the electric quantity between the adjacent points on the line. After discretizing the current $I(l)$ and charge density $\sigma(l)$, the moment solution of the impedance can be represented as:

$$Z_{mn} = j\omega\mu\Delta\overrightarrow{I}_n \cdot \Delta\overrightarrow{I}_m\Psi(m,n) + \frac{1}{j\omega\varepsilon}\left[\Psi\left(\overset{+}{m},\overset{+}{n}\right) - \Psi\left(\overset{+}{m},\overset{-}{n}\right) - \Psi\left(\overset{-}{m},\overset{+}{n}\right) + \Psi\left(\overset{-}{m},\overset{-}{n}\right)\right] \tag{16}$$

where Z_{mn} is the impedance of the antenna on perfect ground. Therefore, the radiation resistance and input reactance can be obtained by $R_r + X_{in} = U_0/I_0$. The electric field $E^i(r)$ can be given as:

$$\begin{bmatrix} f(s_1,s_1') & f(s_1,s_2') & \dots & f(s_1,s_N') \\ f(s_2,s_1') & f(s_2,s_2') & \dots & f(s_2,s_N') \\ \dots & \dots & & \dots \\ f(s_N,s_1') & f(s_N,s_2') & \dots & f(s_N,s_N') \end{bmatrix} \begin{bmatrix} I_1 \\ I_2 \\ \dots \\ I_N \end{bmatrix} = \begin{bmatrix} E_s^i(s_1) \\ E_s^i(s_2) \\ \dots \\ E_s^i(s_N) \end{bmatrix} \tag{17}$$

The discrete values of the current can be obtained by inverting the matrix equation. We can derive the conditions from the convergence of the solution based on the fact that the discrete solution tends to have a stable value as long as the selected segment number N sufficiently large.

3. THE MODEL OF THE VLF UMBRELLA ANTENNA ARRAY

As an example, a VLF umbrella transmitting antenna array is modeled and simulated. The central tower is insulated and has a height of 29 m, and and the bottom of the excitation point is connected to the down-lead wires. As shown in Figure 3(a), the down-lead wires consist of six radiators that have a single copper wire or a cage of six feeding wires. The length of the top wires is 896.5 m. The top wires are covered by tinned copper, shielding the steel wire. Because of the gravity of antenna screen and the pull force of the tower, the position of the connection point of the top wires satisfies the catenary equation [30]. As shown in Figure 3(b),in order to reduce the resistance due to ground loss aground screen consisting of radial grounding wires covering a radius of 1200 m is installed. The ground screen

(a)   (b)
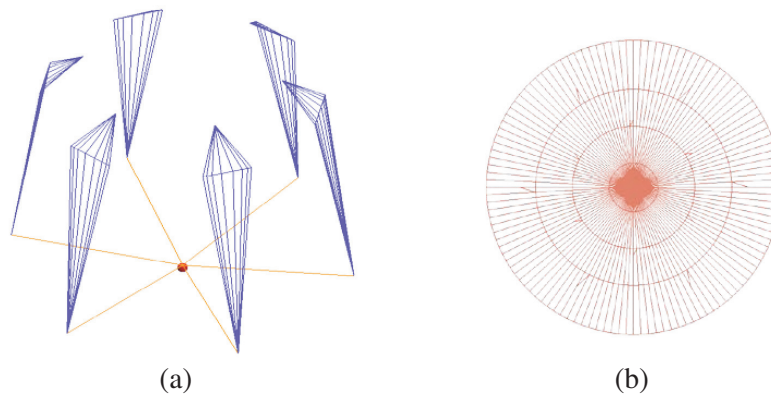
Figure 3. (a) The structure of the down-lead wires in the VLF umbrella transmitting antenna. (b) Ground screen of a VLF umbrella transmitting antenna.

of the model consists of 120 grounding wires with an angle of 3°. The other structural parameters of the VLF model are identical to those described in [31].

The support towers support the top wires, and the towers are insulated from the top wires by high voltage insulators. The tower's height determines the angle between the top wires and the center of the tower. The vertical component of the oblique current present in the top wires generates the electric field. Therefore a small angle will reduce the electric strength of the antenna's vertical electric component.
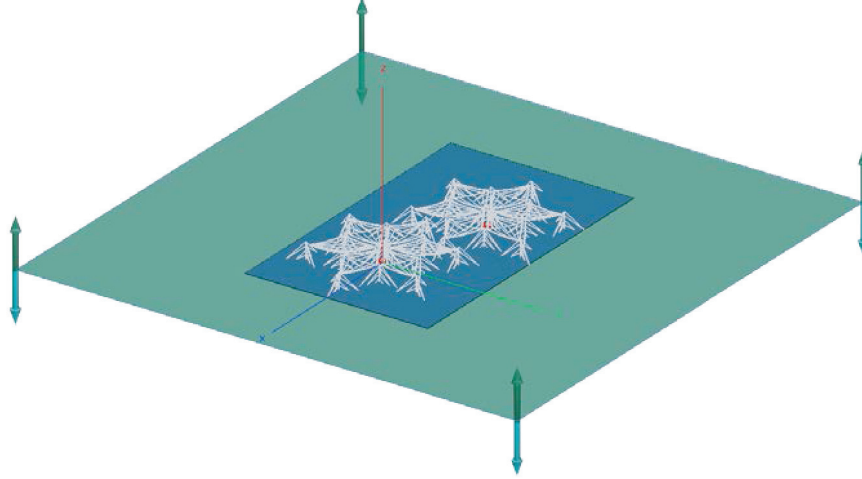
Figure 4. The geometry of the VLF umbrella antenna array on a planar multilayer substrate.

Ground conductivity has a great influence on the radiation efficiency of the VLF transmitting antenna [32]. In the FEKO simulation, we use two types of ground models, homogeneous ground and multilayer substrate ground. The homogeneous ground is a single-layer medium satisfying Green's function. In the multilayer substrate ground, the influence of the ground conductivity on the radiation efficiency of the VLF antenna is considered. As shown in Figure 4 by adding a 4400 m × 2700 m square dielectric block, a multilayer substrate is simulated on the ground in the FEKO software to represent the conductivity of an inhomogeneous ground. The parameters of the multilayer substrate are shown in Table 1.

Table 1. List of the parameters of the multilayer substrate.

	Length	Width	Thickness	Relative permittivity	Relative permeability	Conductivity
Dielectric block	4400 m	2700 m	0.3 m	20	1	0.05 S/m
ground	infinite	infinite	infinite	20	1	0.001 S/m

4. NUMERICAL EXAMPLES

As mentioned above, the mutual coupling of the VLF umbrella array is mainly produced in the radiators of the two array elements. In this study, we evaluate the mutual coupling effect of the VLF umbrella array from two aspects, the array operating modes and the array inter-element spacing.

First, when the grounding condition consists of a planar multilayer substrate, the simulation results in FEKO 7.0 show that the input resistance of the VLF umbrella model with a stand-alone array element operating independently at 24 kHz is 0.279 Ω, and the input reactance is −38.51 Ω. As shown in Table 2,

the radiation resistance is $0.206\,\Omega$, and the radiation resistance of the Cutler measured value of the south array is $0.198\,\Omega$. Due to the differences in the ground dielectric parameters and the grounding screen, the input resistance has a relative error of 5.28%. However, the radiation resistances of the VLF umbrella model are qualitatively similar to those of the Cutler antenna reported in [31]. Therefore, we assume that the antenna model agrees with a practical situation.

Table 2. List of the simulated and measured input impedances of the VLF umbrella antenna array for $f = 24\,\text{kHz}$.

	Input resistance	Input reactance	Radiation resistance
The VLF umbrella model in this study	$0.279\,\Omega$	$-38.51\,\Omega$	$0.206\,\Omega$
The south array of the Cutler measured value in [31]	$0.265\,\Omega$	$-35.40\,\Omega$	$0.198\,\Omega$

4.1. Example One: Impedances in Different Operating Modes

There are two kinds of operating modes for the VLF antenna model configuration. The single feeding mode represents a condition where only one of the two array elements is fed, and in the dual feeding mode, both of array elements are fed simultaneously, forming an active antenna array consisting of the two elements. The feeding ports are located at the bottom of the array elements. Thus, it is noteworthy that a $1\,\text{V}$ voltage source is implemented in the simulations of the VLF model. Because there are many feeding lines and down-leads and they have a thick diameter, it is observed that they have a relatively low loss resistance and contribute little to the input resistance. Therefore, the calculated input resistance does not take into account the loss resistance caused by the feeding lines.

The simulated electrical performances of the VLF umbrella antenna array with the single voltage source are shown in Figure 5. Figure 5(a) and Figure 5(b) clearly show that the input impedances are increasing with the growth of the frequencies. The simulated input impedances are the result of the FEKO simulation that includes the entire coupling structure of the two arrays, while the calculated input impedances are derived by our proposed method. The relative error for the input resistance is less than 6.6% for most of the cases and the maximum error is 14.6% at $10\,\text{kHz}$ frequency. The relative error of the input reactance is less than 10% (Figure 5(b)). Figure 5(b) shows that the input reactance is capacitive, which shows that the VLF umbrella antenna has a higher Q value; the communication frequency band is very narrow. The radiation resistance of the antenna is small and increases slightly as the frequency increases (Figure 5(c)). As expected, the simulated self-resonance frequency of the array antenna is in good agreement with the measured value of the Cutler antenna array, which is about $40\,\text{kHz}$. At a frequency of $24\,\text{kHz}$, the input resistance of the antenna is 2.51% lower than the input resistance of a single thirteen tower umbrella antenna. We assume that the induction current of an indirectly coupled array is low and has little effect on the radiation performance. Moreover, we observe that the system efficiency is greater than 60% at $25\,\text{kHz}$ (Figure 5(d)). Compared with the radiation efficiency at $24\,\text{kHz}$ reported in [31], the simulated efficiency of the VLF umbrella antenna is 0.7% lower than the efficiency of the Cutler's south array, and the calculated efficiency is 7.85% lower than that of the Cutler's at $24\,\text{kHz}$. The main reason of these differences is the difference in the conductivity of the ground.

Figure 6 depicts the electrical parameters of the VLF umbrella antenna array with a dual voltage source. As discussed for the results shown in Figure 5, the consistency between the simulated and calculated input impedances verifies the correctness of the computational method for the coupled VLF antennas as presented in this study. The radiation resistance of the element at the same frequency increases by an average of 96.51% compared to the results shown in Figure 5(c). Compared with the efficiencies shown in Figure 5(d), the simulated radiation efficiency of the element in Figure 6(d) is about 9.17% higher than the radiation efficiency at the same frequency. However, there was no significant increase in the system efficiency for the dual feeding mode above $20\,\text{kHz}$.

4.2. Example Two: Impedances for Different Inter-Element Spacings

The last example is aimed at providing some indications of the impedance effect of mutual coupling for different inter-element spacings of the VLF umbrella antenna array. To control the study variable (e.g., distance), we remove the dielectric block and set the ground conductivity as $0.01\,\mathrm{S/m}$ in this model. The two arrays are fed $1\,\mathrm{V}$ simultaneously, and the following numerical analyses are conducted at the frequency $f = 24\,\mathrm{kHz}$. In order to obtain the electrical parameters, we change the inter-element spacing of the VLF arrays in the EM simulation.

Table 3 shows relatively large differences in the performance of the VLF umbrella antenna arrays located at different inter-element spacings. Compared with the electrical parameters of the modeling array in example one at $24\,\mathrm{kHz}$ (Figure 6), the input impedance and radiation resistance on the homogeneous ground increase (Table 3). However, the radiation efficiency decreases by 8.34%. When the inter-element spacing is less than half of the wavelength ($\lambda = 12.5\,\mathrm{km}$), the radiation efficiency is greater than 50%. Equation (4) shows that the inter-element spacing affects the mutual impedance. In this case, the inter-element spacing d_{12} is smaller than the wavelength and the influence of the direct coupling between the elements is obvious. The mutual coupling interference decreases slightly as the
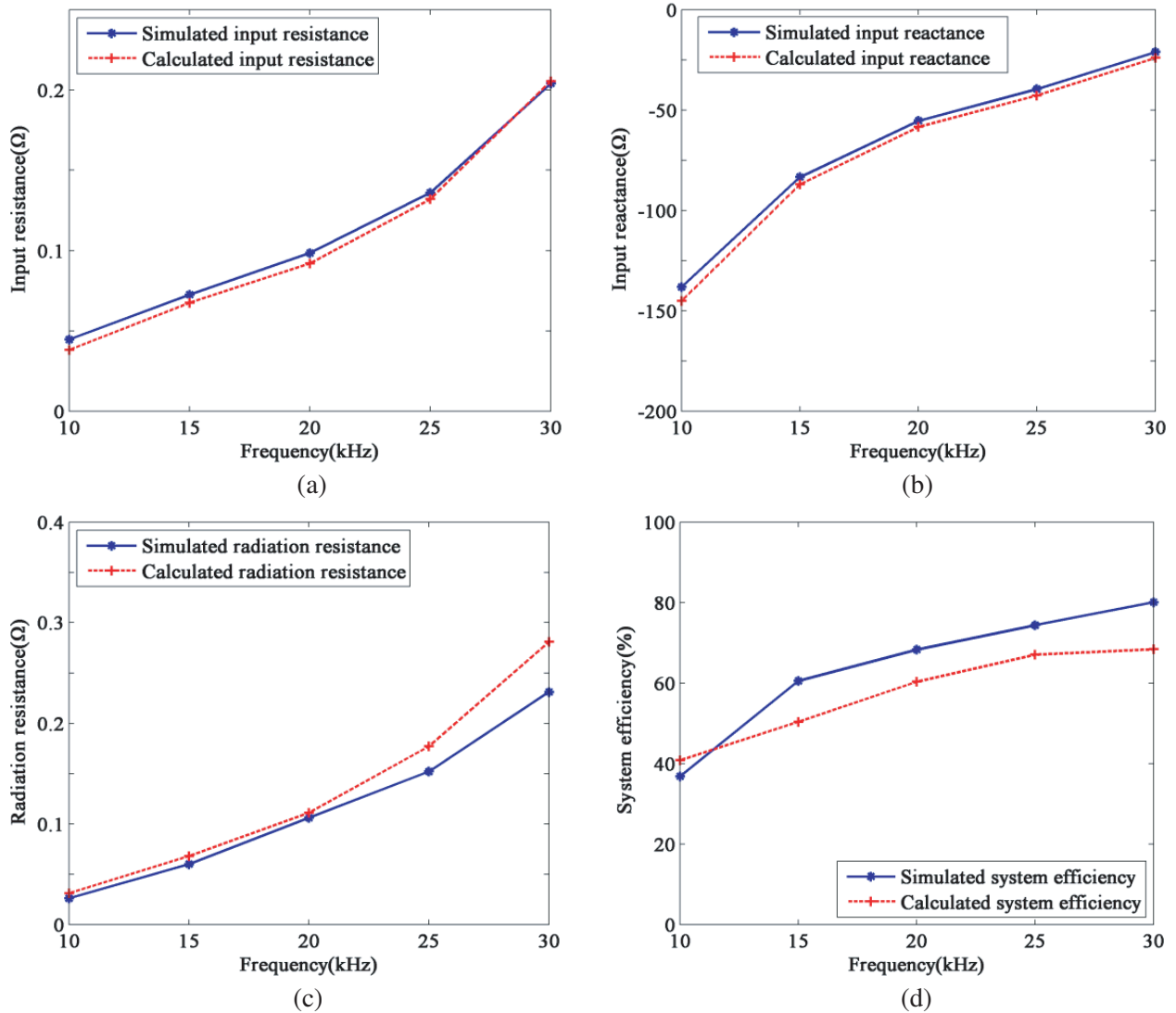
Figure 5. Electrical parameters of the VLF umbrella antenna array with a single voltage source. (a) Input resistance. (b) Input reactance. (c) Radiation resistance. (d) System efficiency.
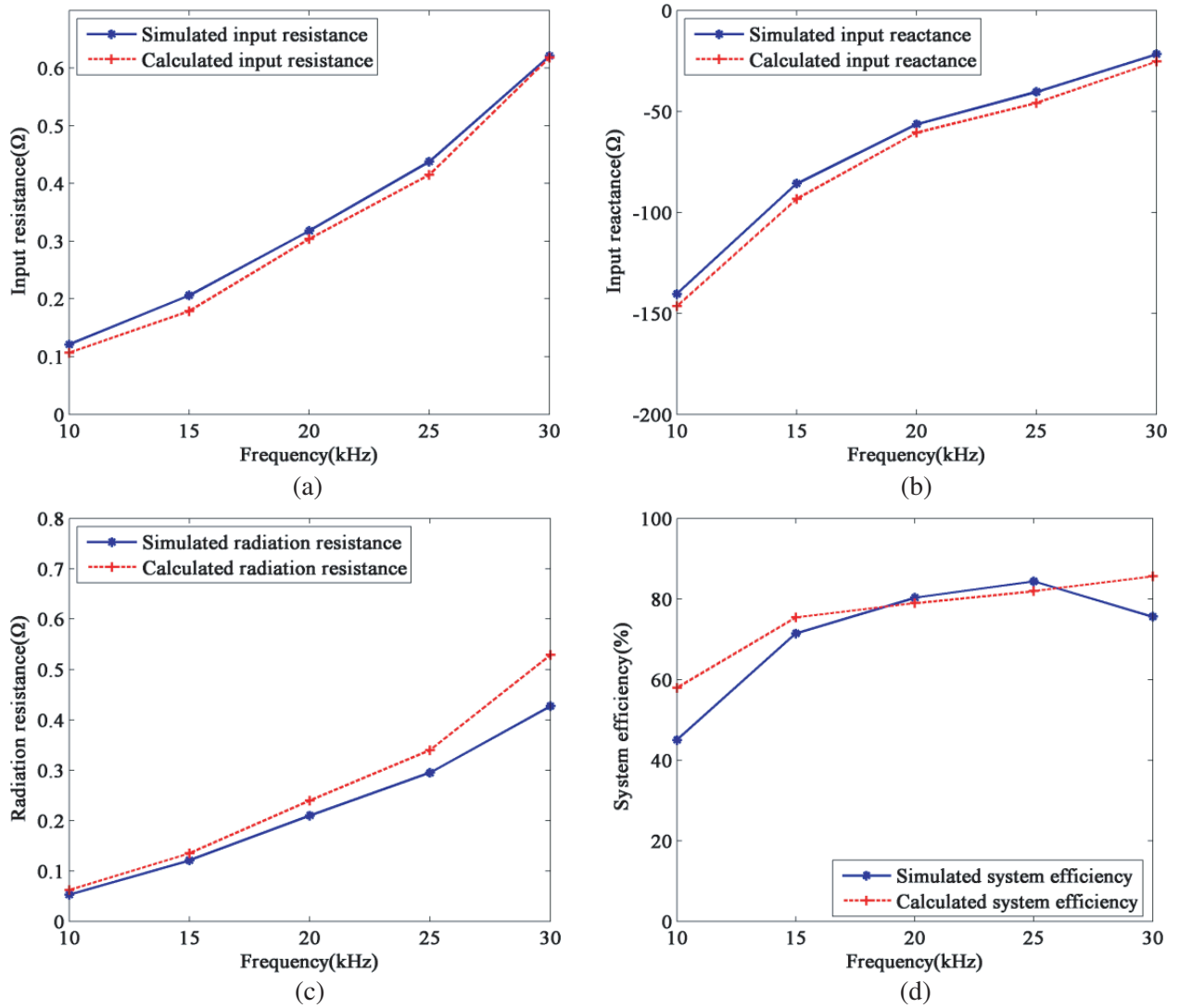
Figure 6. Electrical parameters of the VLF umbrella antenna array with a dual voltage source. (a) Input resistance. (b) Input reactance. (c) Radiation resistance. (d) System efficiency.

spacing increase. It is noteworthy that the radiation patterns of the simulation model show a marked directionality as the inter-element spacing increase (Figure 7), although the wavelength is considerably longer than the spacing. We will discuss the validity and reliability of the phased VLF arrays in a future paper.

Table 3. List of the simulated results of the VLF umbrella antenna array for $f = 24\,\text{kHz}$.

Inter-element spacing	Input resistance	Input reactance	Radiation resistance	Radiation Efficiency
1623 m	0.583 Ω	−37.630 Ω	0.344 Ω	59.01%
3246 m	0.522 Ω	−37.191 Ω	0.295 Ω	56.51%
4869 m	0.434 Ω	−37.172 Ω	0.218 Ω	50.23%
6492 m	0.366 Ω	−37.125 Ω	0.167 Ω	45.63%

| | | | |
| (a) | (b) | (c) | (d) |
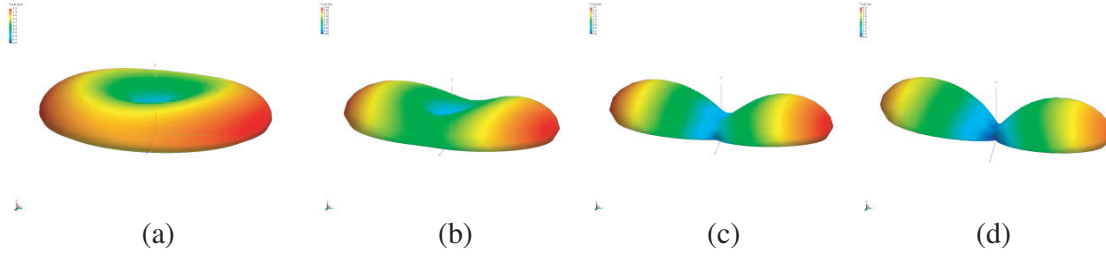
Figure 7. 3D radiation patterns of the VLF model antenna array for different inter-element spacings. (a) $d_{12} = 1623\,\text{m}$, (b) $d_{12} = 3246\,\text{m}$, (c) $d_{12} = 4869\,\text{m}$, (d) $d_{12} = 6492\,\text{m}$.

It is essential to note that neither the material loss resistance nor the ground loss resistance of the towers contributes to the mutual impedance. Therefore, it is unnecessary to consider the loss impedance when analyzing the mutual impedance. Compared with the electrical parameters of the array at 24 kHz in the dual feeding mode, the input impedance and the radiation resistance are increased under uniform ground conditions (Table 3).

5. CONCLUSIONS

In this study, the impedance effect of mutual coupling for a VLF umbrella antenna array is investigated, and an impedance analysis method for the coupled VLF antenna array is developed. Both results suggest that the operation mode and inter-element spacing are two typical factors affecting the impedances of the VLF antenna. In the dual-feeding mode, the direct-mutual coupling results in an increase in the input resistance and a low magnitude of indirect coupling. The relatively small current can help prolong the service life of the VLF antenna. Moreover, compared with the results for dual feeding mode, the radiation resistances clearly decrease for the single feeding mode. However, the loss resistances also decrease in the dual feeding mode, thus, the system efficiency is enhanced. The distance between the VLF umbrella arrays is much smaller than the wavelength for an ESA. When the arrays are placed in close proximity ($kd_{12} < 1$), the effect of mutual impedances is significant. The larger the inter-element spacing of the array is, the smaller the coupling interference is. As for a VLF transmitting antenna array, the method of reducing the mutual coupling is hardly derived from the methods implemented in the HF band or other frequency bands, such as adding parasitic oscillators or sparse optimization by algorithms. When the antenna spacing is properly increased, using different operation frequencies and different feeding modes may reduce the mutual coupling which effects on the electrical performance. The related methods need further investigation. Moreover, by optimizing the tower structure and inter-element spacing to control the mutual coupling interference, it is possible to reduce the ground loss resistance and ensure a high radiation efficiency by increasing the density of the ground grid and selecting sites with low ground resistivity. Compared with other methods, the MoM models are a powerful tool not only for reconciling observed data, but also to make predictions for the performance when certain system parameters are changed (e.g., inter-element spacing) or for an entirely new setting. The proposed method for impedance analysis can be applicable to other kinds of antenna array. Future work in this area will include decreasing the mutual coupling of the bow-tie area, further maximizing the system efficiency of the VLF umbrella arrays, and applying the impedance analysis method to other ESAs.

REFERENCES

1. Li, H.-Y., J. Zhan, Z.-S. Wu, and P. Kong, "Numerical simulations of ELF/VLF wave generated by modulated beat-wave ionospheric heating in high latitude regions," *Progress In Electromagnetics Research M*, Vol. 50, 55–63, 2016.

2. James, M., "Stripping very low frequency communication signals with minimum shift keying encoding from streamed time-domain electromagnetic data," *Geophysics*, Vol. 80, No. 6, 343–353, 2015.

3. Aizebeokhai, A. P. and K. D. Oyeyemi, "Application of geoelectrical resistivity imaging and VLF-EM for subsurface characterization in a sedimentary terrain, Southwestern Nigeria," *Arabian Journal of Geosciences*, Vol. 8, No. 6, 4083–4099, 2015.

4. Hurdsman, D. E., P. M. Hansen, and J. W. Rockway, "LF and VLF antenna modeling," *Antennas and Propagation Society International Symposium*, Vol. 4, 811–814, IEEE, 2003.

5. Liu, C., Q. Z. Liu, L. G Zheng, and W. Yu, "Numeric calculation of input impedance for a giant VLF T-type antenna array," *Progress In Electromagnetics Research*, Vol. 75, 1–10, 2007.

6. Best, S. R., "A discussion on the properties of electrically small self-resonant wire antennas," *IEEE Antennas and Propagation Magazine*, Vol. 46, No. 6, 9–22, 2004

7. Li, H. F. and C. Liu, "Calculation on characteristics of VLF umbrella inverted-cone transmitting antenna," *2014 Sixth International Conference on Ubiquitous and Future Networks (ICUFN)*, 389–391, Shanghai, 2014.

8. Li, H. and C. Liu, "Calculation on characteristics of VLF umbrella inverted-cone transmitting antenna," *International Conference on Ubiquitous & Future Networks*, 389–391, IEEE, July 2014.

9. Dong, Y., C. Liu, G. Dai, and Y. Yan, "VLF transmit antenna impedance characteristic based on top-Load configuration," *Dianbo Kexue Xuebao/Chinese Journal of Radio Science*, Vol. 29, No. 4, 763–768, 2014.

10. Liang, Z. X., H. Xie, Y. Guo, J. Wang, E. P. Li, et al., "Improved hybrid leapfrog ADI-FDTD method for simulating near-field coupling effects among multiple thin wire monopole antennas on a complex platform," *IEEE Transactions on Electromagnetic Compatibility*, Vol. 59, No. 2, 618–626, 2017.

11. Kurs, A., A. Karalis, R. Moffatt, J. D. Joannopoulos, et al., "Wireless power transfer via strongly coupled magnetic resonances," *Science*, Vol. 317, No. 5834, 83–86, AAAS, 2007.

12. Huang, Q., H. Zhou, and X.-W. Shi, "A new compensating method for the mutual coupling effect in adaptive antenna arrays composed of wire elements," *Progress In Electromagnetics Research C*, Vol. 35, 221–236, 2013.

13. Youndo, T., P. Jongmin, and N. Sangwook, "Mode-based analysis of resonant characteristics for near-field coupled small antennas," *IEEE Antennas and Wireless Propagation Letters*, Vol. 8, No. 4, 1238–1241, IEEE, 2009.

14. Fallahi, R. and M. Roshandel, "Effect of mutual coupling and configuration of concentric circular array antenna on the signal-to-interference performance in CDMA systems," *Progress In Electromagnetics Research*, Vol. 76, 427–447, 2007.

15. Liao, B. and S. C. Chan, "A cumulant-based method for direction finding in uniform linear array with mutual coupling," *IEEE Antennas and Wireless Propagation Letters*, Vol. 13, 1717–1720, IEEE, August 2014.

16. Gupta, I. J. and A. A. Ksienski, "Effect of mutual coupling on the performance of adaptive arrays," *IEEE Transactions on Antennas and Propagation*, Vol. 31, No. 5, 785–791, September 1983.

17. Su, T. and L. Hao, "On modeling mutual coupling in antenna arrays using the coupling matrix," *Microwave and Optical Technology Letters*, Vol. 28, No. 4, 232–237, February 2001.

18. Ralchenko, M., M. Roper, M. Svilans, and C. Samson, "Coupling of very low frequency through-the-Earth radio signals to elongated conductors," *IEEE Transactions on Antennas and Propagation*, Vol. 65, No. 6, 3146–3153, 2017.

19. Balanis, C. A., *Antenna Theory: Analysis and Design*, 4th edition, Wiley Press, Hoboken, 2016.

20. Rueda, C. I. P. and R. B. Miller, "A new approximate closed solution for small dipole antenna with method of moments," *IEEE Latin America Transactions*, Vol. 14, No. 4, 1562–1569, IEEE, 2016.

21. He, Q. Q. and B. Z.Wang, "Design of microstrip array antenna by using active element pattern technique combining with Taylor synthesis method," *Progress In Electromagnetics Research*, Vol. 80, 63–76, 2008.

22. Carlo, F. M. C. and B. Alessio, "Electromotive force induced in and inductance of an electrically small circular loop antenna," *IEEE Transactions on Electromagnetic Compatibility*, Vol. 56, No. 4, 780–783, August 2014.

23. Carobbi, C. F. M. and A. Bonci, "Electromotive force induced in and inductance of an electrically small circular loop antenna," *IEEE Transactions on Electromagnetic Compatibility*, Vol. 56, No. 4, 780–783, 2012.

24. Liu, C., H. Jiang, and J. H. Huang, *Very Low Frequency Communication*, Haichao Press, Beijing, 2008.

25. Jobava, R. G., A. L. Gheonjian, J. Hippeli, G. Chiqovani, D. D. Karkashadze, et al., "Simulation of low-frequency magnetic fields in automotive EMC problems," *IEEE Transactions on Electromagnetic Compatibility*, Vol. 56, No. 6, 1420–1430, 2014.

26. Taylor, D. and P. Loschialpo, "Imaging of helical surface wavemodes in the near field," *Journal of Electromagnetic Waves and Application*, Vol. 17, No. 11, 1593–1604, 2003.

27. Ubeda, E., J. M.Rius, and A. Heldring, "Nonconforming discretization of the electric-field integral equation for closed perfectly conducting objects," *IEEE Transactions on Antennas and Propagation*, Vol. 62, No. 8, 4171–4186, 2014.

28. Miller, E. K. and F. J. Dearick, "Some computational aspects of thin-wire modeling," *Numerical and Asymptotic Techniques in Electromagnetics*, Vol. 3, 89–127, Springer-Verlag, New York, July 2005.

29. Hatamzadeh-Varmazyar, S., M. Naser-Moghadasi, and Z. Masouri, "A moment method simulation of electromagnetic scattering from conducting bodies," *Progress In Electromagnetics Research*, Vol. 81, 99–119, 2008.

30. Huang, Q. L., *Electrical Power Engineer's Handbook*, China Electric Power Press, Beijing, 2002.

31. Hansen, P. and J. Chavez, *VLF Cutler: September 1997, Four-Panel Tests; RADHAZ and Field Strength Measurement*, Space and Naval Warfare Systems Center, San Diego, 1997.

32. Hansen, P., "Terrestrial antenna for high power VLF radiation into the magnetosphere," *General Assembly and Scientific Symposium (URSI GASS)*, 1–4, Beijing, 2014.